

# Input Separability in Living Liquid State Machines

Robert L. Ortman<sup>1,3</sup>, Kumar Venayagamoorthy<sup>4</sup>, and Steve M. Potter<sup>1,2</sup>

<sup>1</sup>Laboratory for Neuroengineering, Georgia Institute of Technology

<sup>2</sup>Coulter Department of Biomedical Engineering, Georgia Institute of Technology

<sup>3</sup>School of Electrical and Computer Engineering, Georgia Institute of Technology,  
313 Ferst Dr., Atlanta, GA 30313, USA

<sup>4</sup>Real-Time Power and Intelligent Systems Laboratory,  
Missouri University of Science and Technology,  
1870 Miner Circle, Rolla, MO 65409, USA  
rlortman@gatech.edu, ganeshv@mst.edu,  
steve.potter@bme.gatech.edu

**Abstract.** To further understand computation in living neuronal networks (LNNs) and improve artificial neural networks (ANNs), we seek to create a hybrid liquid state machine (LSM) that relies on an LNN for the reservoir. This study embarks on a crucial first step, establishing effective methods for finding large numbers of separable input stimulation patterns in LNNs. The separation property is essential for information transfer to LSMs and therefore necessary for computation in our hybrid system. In order to successfully transfer information to the reservoir, it must be encoded into stimuli that reliably evoke separable responses. Candidate spatio-temporal patterns are delivered to LNNs via microelectrode arrays (MEAs), and the separability of their corresponding responses is assessed. Support vector machine (SVM) classifiers assess separability and a genetic algorithm-based method identifies subsets of maximally separable patterns. The tradeoff between symbol set size and separability is evaluated.

**Keywords:** Separation property, cultured neuronal network, liquid state machine, support vector machine, microelectrode array.

## 1 Introduction

The central nervous system of complex organisms is well known to effectively handle complex computational problems such as pattern recognition and non-linear control, having an unmatched ability to adapt in real time to changing environmental cues. The most advanced artificial neural networks (ANNs) have yet to rival the computational performance of simple brains for certain types of problems, leaving vast potential for improvement of ANNs if their living counterparts can be better understood. While the nervous system has been examined on a multitude of scales, including the single-neuron level and the whole-brain level, only recently have neuroscientists and neuro engineers had the ability to study neurons on the small network level. This has been done by plating living neuronal cultures, known as living neuronal networks (LNNs), on microelectrode arrays (MEAs), forming a bi-directional interface between

living neurons and computer systems. Electrodes embedded in the MEA substrate allow cultures to be monitored and stimulated for extended periods of time [1].

### 1.1 Motivation

This research embarks on preliminary steps necessary to enable advanced future studies of network learning and computational mechanisms in closed-loop hybrid neural micro-systems. The external computer system interfaced to the LNN can send and receive arbitrary sensory and motor information to and from the LNN, limited only by the maximum data rate to which the LNN can respond and generate meaningful responses.

Identifying a set of input stimulation patterns for a specific LNN that achieves an optimal tradeoff between raw data rate and separability is therefore of paramount importance. While previous studies of hybrid computational systems using *in vitro* LNNs have been limited to very low input/output rates and simple computational tasks with static goals, we aspire to perform far more advanced computations, including the control of complex dynamical systems. Past research by the authors includes the use of multi-electrode stimuli to train an LNN to control the behavior of a simulated animal (animat) in a goal-directed navigation task [2].

Current research aims to examine the ability of hybrid LNN-based systems to accurately predict and control non-linear, non-stationary dynamical systems, including simulated power systems (NSF EFRI-COPN Project #0836017). Other studies have applied NNs and advanced computational techniques to identification, control, and optimization of power systems and achieved promising results [3]. However, NNs have not been able to achieve the degree of optimal control and significant scalability evident in biological networks. Knowledge gained from studying LNNs can be exploited to better emulate their behavior in next generation NNs and produce vastly superior computational systems.

### 1.2 Neuronal Cell Cultures

Cells from E18 (embryotic day 18) rat cortices (supplied by BrainBits<sup>®</sup>, Springfield, IL, USA) were enzymatically and mechanically dissociated to obtain a target density of approximately 2500 cell/ $\mu$ L of medium and then layered onto laminin-coated 60-electrode (59 recording/stimulation electrodes plus one ground) Multichannel Systems MEAs (30  $\mu$ m diameter titanium nitride electrodes in a square grid with 200  $\mu$ m spacing) [2]. Cells were plated and grown in Jimbo's medium (containing 10% equine serum, sodium pyruvate, insulin, and GlutaMAX<sup>™</sup>) [4] [5]. When not in use, the LNNs were stored in an incubator at 35°C with 5% CO<sub>2</sub>, 9% O<sub>2</sub>, and 65% relative humidity in Teflon<sup>®</sup>-membrane sealed MEAs [6]. Experiments were performed during three to five weeks *in vitro* on cultures of approximately 20 000 living neurons.

### 1.3 Data Acquisition and Stimulation System

Our customized electrophysiology system, NeuroRighter<sup>™</sup> [7] [8] allows for versatile low-latency closed-loop experiments. The hardware for stimulation and recording includes a Multichannel Systems MEA60 preamp to which the MEA directly connects. The amplified MEA output, containing neural signals, passes through custom signal conditioning interface boards before terminating onto two National Instruments<sup>™</sup> (NI)

PCIe-6259 data acquisition cards (32 analog input channels each) installed in a PC. The stimulation output originates from the computer from a PCIe-6259 card via its four analog outputs and then passes through custom interface boards, multiplexer headstages, and finally into the MEA. The PCIe-6259 cards' digital outputs are used to control the multiplexers. Independent recording and stimulation is possible from all 59 electrodes.

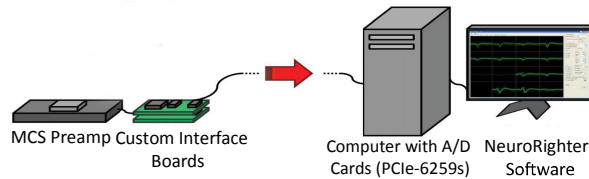


**Fig. 1.** NeuroRighter System

The stimulation and recording protocol was programmed as a plug-in for NeuroRighter and is written in C#. The DAQ cards are controlled by the NeuroRighter software via NI Measurement Studio™ using NI DAQmx drivers.

## 2 Living Reservoir LSM Experiment

Previous research has demonstrated that the LSM model provides an excellent framework for inducing computation in excitable dynamical systems, referred to as reservoirs, such as biological neuronal networks [9]. Typical LSM research uses an NN as the reservoir, but recently the behavior of systems utilizing *in vitro* LNNs as a reservoir has been studied [11] [12]. Our experiments investigate the essential separation property for large numbers of input stimuli in a living reservoir LSM.

### 2.1 Method Details

Each input symbol was represented as a stimulation pattern defined by a specific sequence of four electrodes and a particular interpulse frequency. Data was collected from two different LNNs using stimulus pattern sets composed of 48 unique symbols (patterns). The maximally separable subsets of length two through approximately 25 were computed for each experimental data set using the methods described in Section 3. Patterns were tested in random order to minimize the effects of any potential short-term plasticity. Biphasic square pulses 0.6 V peak-to-peak, 800  $\mu$ s long were used.

From the 59 MEA electrodes, 32 stimulation electrodes were chosen at random from the subset found to evoke responses in a preliminary electrode screening procedure executed in NeuroRighter. The 32 stimulation electrodes were further subdivided into eight randomly chosen, non-overlapping groups of four electrodes each. In addition, six stimulation frequencies were selected in uniform steps between 15 Hz and 40 Hz (inclusive), yielding a total of 48 individual symbols. Each symbol set was tested using uniformly distributed random symbol input files with 1083 total symbol stimulations,

corresponding to about five minutes of real-time per experiment. Consequently each unique pattern was tried about 23 times in a given experiment. Twenty such experiments were performed on each of the two LNNs.

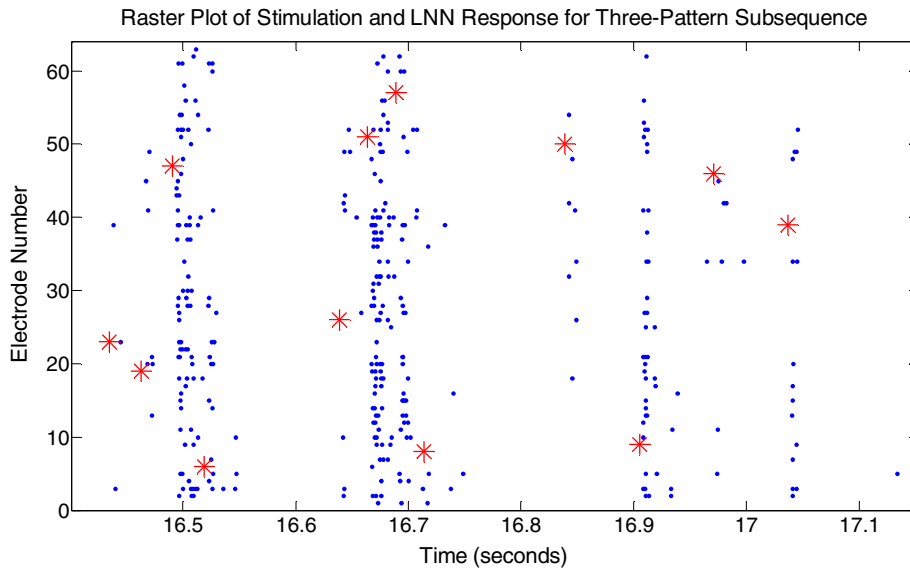


**Fig. 2.** The plot above shows three stimulation patterns (symbols) being delivered to the LNN and their corresponding responses. The red asterisk symbols mark the times and electrode numbers on which stimulation occurred. The three input patterns shown here all differ in both spatial region (electrode set) and frequency. The blue dots indicate detected spikes after artifact removal.

### 2.2 Classification of LNN Responses to Sensory Input

Stimulation patterns (symbols) were interleaved with quiet (non-stimulation) periods. Pattern time length varied from approximately 100–300 ms (depending on frequency), and inter-symbol delay was fixed to 100 ms. Pattern parameters were chosen such that the mean stimulation frequency across the entire MEA was constrained to be approximately 20 Hz in order to prevent bursting activity that would disrupt meaningful responses [10].

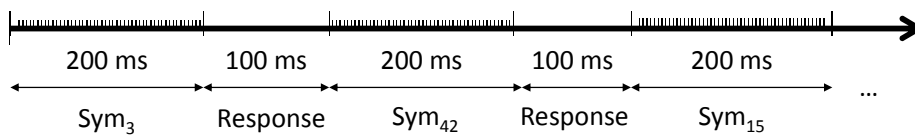


**Fig. 3.** The figure above is a graphical representation of the interleaved stimulation and response phase architecture described in this section. The times given are approximate mean durations for the different phases. Each Sym<sub>x</sub> indicates stimulation with a randomly chosen symbol (pattern) from the set of 48.

During the non-stimulation period following each input symbol, the recorded spike activity was passed through a leaky integrator function, (1), producing the liquid state output. The output was subsequently sampled at 16 evenly spaced intervals five ms apart. Such an approach is based on commonly used techniques for extracting responses from LSMs and LNNs [11] [12].

$$x_i(t) = \sum_{s_i} e^{-(t-s_i)/\tau} \quad (1)$$

In (1),  $x_i(t)$  are the values of the liquid state readout function over time for electrode  $i$ , and the  $s_i$  values are the time stamps designating when spikes were detected during the response period for a particular electrode. Time is represented by  $t$ ; the time constant,  $\tau = 60$  ms, limits the memory of the output.

Each stimulation trial corresponds to 59 liquid state outputs, one per electrode. Since each electrode's integrator output is represented by 16 samples, every response is represented as a 944-dimensional vector.

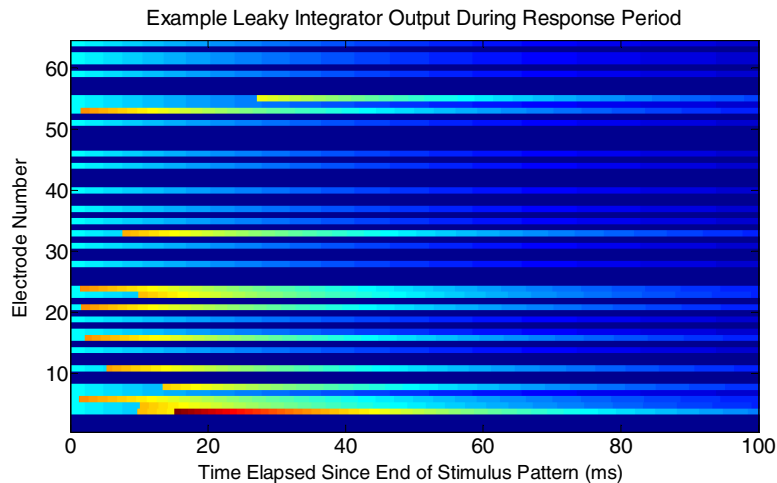


**Fig. 4.** The figure shows an example liquid state output from the leaky integrator in response to neuronal spikes recorded following a stimulation pattern (stimulus not shown). Liquid state output voltage is represented by color, with red indicating highest voltage and dark blue indicating zero. The time constant is 60 ms. Such responses are computed for every trial of each pattern and then sampled (as described above) to produce the input data for the classifier.

### 2.3 Stimulus Artifact Suppression Techniques

Stimulus artifacts present a formidable obstacle to reliable data collection and analysis for these types of experiments. Several techniques are used to ensure recorded results reflect actual neuronal activity. NeuroRighter incorporates band pass filtering and thresholding to detect spikes. In addition, NeuroRighter includes post processing

using the SALPA algorithm [8], a variable time-constant polynomial curve fit used to subtract large voltage changes due to stimulation [13].

The real-time SALPA (subtraction of artifacts by local polynomial approximation) algorithm in NeuroRighter effectively suppresses a large amount of stimulation artifacts [8] [13] but some still remain. Further post-processing of data removes spikes with greater than 300  $\mu$ V peak-peak amplitudes. Finally, offline waveform clustering software is used to cluster spike response waveforms into up to 192 units [14]. Spikes belonging to the units whose average waveform deviates greatly from valid spike waveforms are removed. For typical data sets, 20% of spikes detected by NeuroRighter were eliminated by the clustering approach.

### 3 Response Classification and Determination of Separable Pattern Subsets

Offline analysis software was used for detection of stimulus patterns given the liquid state responses described in Section 2.2. The open source support vector machine (SVM) package, LIBSVM, was used to solve the multiclass SVM detection problem [15]. Training was performed on 33% of the data, and classification was attempted on the remaining 67%. Repeated random sub-sampling cross-validation was used in order to eliminate the bias that might occur from only choosing one random training and classification set [15] [16]. The cross-validation reduces variance and protects against Type III statistical errors [17]. After the first training and testing iteration, the training and classification groups were randomly reselected, new support vectors were trained, and classification was attempted with the same approach as before. This process was repeated for 50 trial iterations, and the overall mean performance was calculated. Fifty iterations were used because increasing iteration count beyond 20-50 (depending on the data set) produced no further statistically significant reduction in the standard deviation of results.

Performance was evaluated by mean classification accuracy for each particular set of patterns evaluated. Classification accuracy ( $1 - \text{probability of symbol error}$ ) is defined as the ratio of the number of symbols correctly identified by the classifier out of the total number tested.

#### 3.1 Classifier Parameter Optimization

Leaky integration and SVM parameters were varied to optimize detection. The time constant,  $\tau$ , was varied over a range of 5-100ms, and 60 ms was found to be generally optimal. The number of samples taken between zero and 80 ms of the leaky integrated response period response was varied between one and 32, inclusive, in powers of two. Accuracy increased with increasing number of samples until about eight, above which improvements substantially diminished. A setting of 16 samples was chosen since no classification performance improvement was observed beyond 16 samples, and more samples (therefore more SVM input features) significantly increases computation time and memory requirements.

The SVM kernel and corresponding parameters were also optimized for best classification accuracy. The kernels evaluated were linear, quadratic, third-order polynomial, fourth-order polynomial, radial basis functions, and sigmoid (multilayer perceptron (MLP)). The sigmoid kernel (2) was selected since it produced the best results. The training data vectors comprise  $u$  and  $v$ , and the kernel parameters are given by  $\gamma$  and  $C_0$ . The optimal parameters were found to be as follows:  $C = 16$  (cost parameter of C-SVC SVM),  $\gamma = (1 / \text{number of features}) = 1/944$ , and  $C_0 = 0$ .

$$\tanh(\gamma u'v + C_0) \quad (2)$$

### 3.2 Genetic Algorithm-Based Approach for Finding Best Pattern Subsets

From each initial candidate set of 48 patterns, we sought an algorithmic approach for finding the most separable pattern subset of varying sizes in an effort to construct subsets corresponding to the greatest net bit rate (occurring at the optimal tradeoff between maximizing symbol set size and minimizing error probability). The chosen technique, based on genetic algorithms [18], was found to be highly effective.

For each data set, some of the candidate patterns were found to evoke far more complex and reliable responses than others. Patterns evoking no response in the LNN for more than 33% of their trials were excluded at the start of the algorithm. Size  $n$  subsets of the most separable patterns were determined from the remaining patterns in the following manner: First, separability between all pairwise combinations ( $n = 2$ ) of the remaining patterns was assessed. The top 5% most separable subsets were selected to serve as the basis for forming the next generation, pattern subsets of size  $n = 3$ . This process was repeated until subset size reached the total number of usable patterns (typically about 20-25 of the original 48).

The metric, classification accuracy, was used as the fitness function. Next generation candidate pattern sets of  $(n + 1)$  patterns were bred from the most separable 5% of the size  $n$  subsets by appending a single additional pattern chosen from the set of those whose fitness was in the best 10% of pattern subsets of size two. All possible combinations of new candidate subsets subject to these fitness constraints (the next generation) were formed and evaluated, and the process was repeated to produce the subsequent generations.

### 3.3 Results

The plots below show the results for maximally separable stimulus pattern (symbol) subsets based on data from the two different LNNs. Separability is indicated by mean classifier performance ( $1 - \text{probability of error}$ ) for the chosen patterns and data set. The results portray the best pattern sets determined for the two LNNs. Based on these data, one could reasonably expect to transfer data into the living reservoir LNNs used in our experiments at a rate of approximately one byte per second.

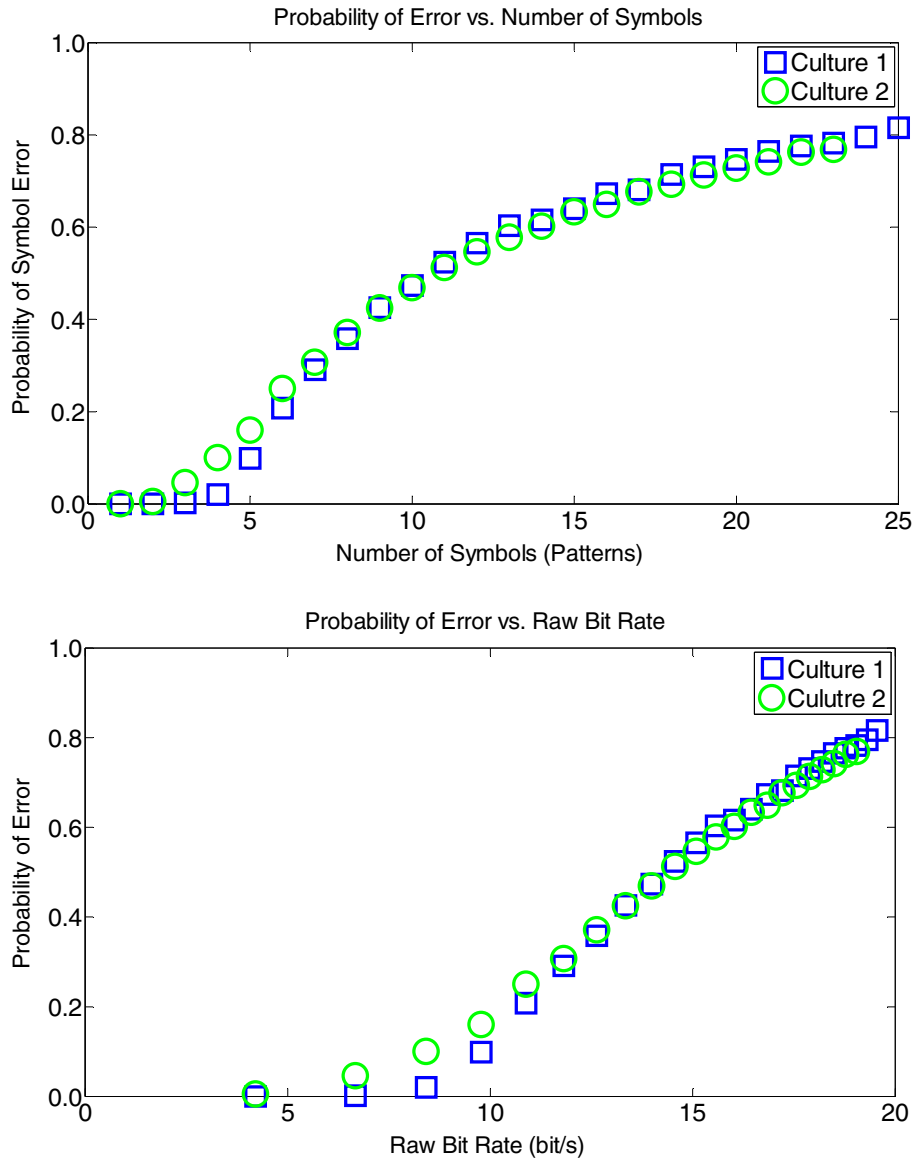


**Fig. 5.** The above plots show performance for the system as it varies with the number of distinct patterns (symbols) and corresponding bit rate. Results for two LNNs, labeled Culture 1 and Culture 2, are displayed.

#### 4 Conclusions and Future Work

The results show that substantially separable input patterns can be found, and in future experiments, greater performance is expected. Given the present results, we can

expect to transfer input data to the LNNs at a rate of about one byte per second. Such performance is useful for certain types of potential *invitro* learning experiments but falls short of that expected given better MEAs, cultures, and coding schemes.

Of the two cultures used in these experiments, one of them produced reliable recordings from only one-fifth to one-fourth of its electrodes due to a combination of MEA electrode failure and culture death. The other LNN exhibited pathological bursting that often could not be consistently suppressed. In subsequent studies, we plan to collect data from large numbers of high quality LNNs plated on fully functional MEAs and use a wider range of stimulus patterns.

In addition to SVM-based classification, other approaches may be explored for assessing separability. In upcoming experiments, stimulation patterns will be optimized online during experiments via a closed-loop stimulation pattern plug-in for Neuro-Righter. We also seek to identify which stimulus pattern parameters correlate with greater separability and reliability over large time scales (hours to days).

#### 4.1 Closed-Loop Input Pattern Separability Optimization

Although these experiments were successful in finding some highly separable pattern sets, the patterns were found much later than the experiments on the living cultures that responded to them. This is problematic for future computational experiments, since we aim to find separable patterns and subsequently use them to transfer sensory input to the LNNs: Since living neuronal networks are highly dynamic over time, even the most reliable patterns may not be effective at later times. Separable patterns must ideally be found just prior to a learning experiment and their performance frequently reevaluated over time.

With a closed-loop system, candidate patterns will be tested on live cultures and analyzed online for separability using variants of the methods previously described. Ineffective patterns will be eliminated and replaced with new patterns. The process will repeat until pattern sets are found that achieve the net bit rate required for a particular experiment. The sets' effectiveness can be monitored over time, and patterns can be adjusted in an attempt to maintain successful communication.

#### 4.2 Characteristics of Separable Patterns

Analysis of the electrode subsets and frequencies corresponding to the most and least separable patterns for an LNN is ongoing. Preliminary results show that a large difference between spatial positions of electrodes is much more correlated with high separability than difference in frequency between patterns.

We intend to analyze performance with respect to each pattern's frequency, electrode impedances, spatial locations in the MEA, and other parameters in an effort to determine which characteristics correlate with high reliability and separability.

**Acknowledgments.** This work is supported under a grant from the National Science Foundation, "Neuroscience and Neural Networks for Engineering the Future Intelligent Electric Power Grid," as part of the Emerging Frontiers in Research and Innovation (EFRI) program for Cognitive Optimization and Prediction (COPN) projects, NSF EFRI-COPN Grant #0836017.

## References

1. Taketani, M., Baudry, M.: *Advances in Network Electrophysiology Using Multi-Electrode Arrays*. Springer, Heidelberg (2006)
2. Bakkum, D.J., Chao, Z.C., Potter, S.M.: Spatio-Temporal Electrical Stimuli Shape Behavior of an Embodied Cortical Network in a Goal-Directed Learning Task. *J. Neur. Eng.*, 310–323 (2008)
3. Park, J., Harley, R., Venayagamoorthy, G.: Adaptive Critic Based Optimal Neurocontrol for Synchronous Generator in Power System Using MLP/RBF Neural Networks. *IEEE Trans. on Industry Applications* 39(5) (2003)
4. Potter, S.M., Wagenaar, D.A., DeMarse, T.B.: Closing the Loop: Stimulation Feedback Systems for Embodied MEA Cultures (2001)
5. Wagenaar, D.A.: Persistent Dynamic Attractors in Activity Patterns of Cultured Neuronal Networks. *Phys. Rev. E* 73(5) (2006)
6. Potter, S.M., DeMarse, T.B.: A New Approach to Neural Cell Culture for Long-Term Studies. *J. Neurosci. Methods* 110, 17–24 (2001)
7. Rolston, J.: *Creating NeuroRighter* (2009), <http://groups.google.com/group/neurorightter-users>
8. Rolston, J.D., Gross, R.E., Potter, S.M.: A Low-Cost Multielectrode System for Data Acquisition Enabling Real-Time Closed-Loop Processing with Rapid Recovery from Stimulation Artifacts. *Frontiers in Neuroengineering* 2(12), 1–17 (2009)
9. Maass, W., Natschlaeger, T., Markram, H.: A model for real-time computation in Generic Neural Microcircuits. *Adv. Neural Info. Proc. Sys.* 15, 229–236 (2003)
10. Wagenaar, D.A., Madhavan, R., Potter, S.M.: Controlling Bursting in Cortical Cultures with Multi-Electrode Stimulation. *J. Neurosci.* 25(3), 680–688 (2005)
11. Hafizovic, S., Heer, F., et al.: A CMOS-Based Microelectrode Array for Interaction with Neuronal Cultures. *J. Neurosci. Methods*, 93–106 (2007)
12. Dockendorf, K.P., Park, I.: Liquid State Machines and Cultured Cortical Networks: The Separation Property. *Biosystems* 95, 90–97 (2009)
13. Wagenaar, D.A., Potter, S.M.: Real-Time Multi-Channel Stimulus Artifact Suppression by Local Curve Fitting. *J. Neurosci. Methods* 120, 113–120 (2002)
14. QuianQuiroga, R., Nadasdy, Z., Ben-Shaul, Y.: Unsupervised Spike Detection and Sorting with Wavelets and Superparamagnetic Clustering. *Neural Comput.* 16, 1661–1687 (2004)
15. Chang, C.-C., Lin, C.-J.: LIBSVM: A Library for Support Vector Machines (2001), <http://www.csie.ntu.edu.tw/~cjlin/libsvm> (September 2010) release
16. Geisser, S.: *Predictive Inference*, New York (1993)
17. Mosteller, F.: A  $k$ -sample Slippage Test for an Extreme Population. *Annals of Mathematical Statistics* 19(1), 58–65 (1948)
18. Fraser, A.S.: Simulation of Genetic Systems by Automatic Digital Computers. *Australian Journal of Bio. Sci.* 10, 484–491 (1957)